BOLETIN DE LA SOCIEDAD ESPAÑOLA DE
Cerámica y Vidrio
www.elsevier.es/bsecv

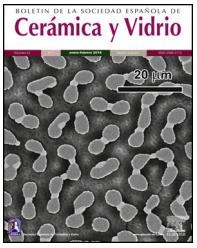

Further characterization of the surface properties of the SiC particles through complementarity of XPS and IGC-ID techniques

*Aitana Tamayo**, *Fausto Rubio*, *Maria Alejandra Mazo*, *Juan Rubio*

Ceramics and Glass Institute, CSIC, Madrid, Spain

ARTICLE INFO

Article history:
Received 12 September 2017
Accepted 20 April 2018
Available online 5 May 2018

Keywords:
XPS
IGC-ID
SiC
Surface properties

ABSTRACT

In this work we demonstrated the necessity to complement the techniques XPS and IGC-ID to evaluate the surface properties of the SiC materials. We have studied four SiC materials with different particles sizes being 3 of them of a Si/C ratio close to the stoichiometry whereas for the fourth one, this ratio is 0.7, indicating an excess of C in the surface of the particles. The dispersive energy, γ_s^d, of these materials is 77.5, 64.0, 40.5 and 44.5 for the SiC sized 0.7, 1, 7 and 10 μm, respectively. The lowest γ_s^d values are found for the SiC than in XPS presented an excess of surface carbon. The acid constants k_A are close to unity and in the case of the base constant k_B, they are found to be 1.1, 1.0, 0.4 and 1.1 for each above mentioned particle sized, being again the sample that presented the lowest k_B value the sample that presented a particle size of 0.7. The SiC with an excess of surface C presents the lowest k_B/k_A ratio indicating that most part of the active sites are blocked by carbon atoms.

Caracterización completa de las propiedades superficiales de partículas de SiC mediante complementariedad de las técnicas XPS e IGC-ID

Palabras clave:
XPS
IGC-ID
SiC
Propiedades superficiales

RESUMEN

En este trabajo se ha mostrado cómo las técnicas XPS e IGC-ID son complementarias a la hora de evaluar las propiedades superficiales de partículas de SiC. De los cuatro SiC analizados tres de ellos poseen una relación Si/C próxima a la estequiométrica, mientras que en el otro caso dicha relación es de 0.7, indicando un exceso en C superficial. La energía dispersiva γ_s^d de estos materiales presenta valores de 77.5, 64.0, 40.3 y 44.5 para los SiC de 0.7, 1, 7 y 10 micrómetros de tamaño de partícula, siendo inferior para aquel SiC que por XPS presenta la relación Si/C de 0.7. Las constantes ácidas k_A poseen valores de 1.01, 0.98, 1.10 y 1.00, a la vez que las constantes básicas k_B son de 1.1, 1.0, 0.4 y 1.1, para los SiC de 0.7, 1, 7 y 10 micrómetros, respectivamente. De nuevo se comprueba que el SiC con exceso de C presenta un valor más pequeño de la relación k_B/k_A indicando que gran parte de los centros activos están bloqueados por carbono.

* *Corresponding author.*
E-mail address: aitanath@icv.csic.es (A. Tamayo).
https://doi.org/10.1016/j.bsecv.2018.04.003

Introduction

Over the later years, ceramic materials are been considered as advanced materials because their multiple applications either at low, medium or high temperatures even in very harsh environments. The versatility of the ceramic materials is however limited due to the intrinsic problematics of the actual synthetic methodologies or processing techniques. Most of the high-temperature materials (such as SiC or Si_3N_4) are covalent solids where a large number of electrons are shared between atoms. Ionic solids such as TiO_2, ZrO_2, MgO or BeO possess a marked electronegativity difference and thus, they also possess high melting points. Compounds that are either mostly ionic or mostly covalent have higher melting points than compounds in which neither kind of bonding predominates and their overall properties depend on the dominant bonding mechanism. Because of the high strength of the shared bonds in refractory materials, during grinding to very low particle sizes, the particles obtained possess highly reactive surfaces. This reactivity is related to the large number of broken bonds formed between atoms located at the surface of the particles. Contrary to bulk atoms, whose valences are fully compensated, the broken surface bonds are restored by forming distorted bridges but still, some of them remain uncompensated. If the solids are processed in air, the unbalanced valences will react with the environmental atmosphere and thus, water vapor will form hydroxilic species of a Brönsted acid nature. Besides, the nature of the ceramic materials, the synthetic route (sol–gel, combustion synthesis, coprecipitation, thermal decomposition, etc.), crystallinity and thermal background conform a wide variability of parameters of a high importance that will determine the surface properties of a ceramic material in particular.

The active centers of the covalent solids are mainly hydroxyl sites or other nitrogenated groups such as $–NH_2$. These active sites can be also produced by tensioned or distorted bridges which can be opened and react through multiple chemical reactions. Broken bonds and atoms with non-compensated valences coexist with radicals originated by atmosphere-driven reactions on the surface of grinded solids. $SiOO^-$ terminations are highly reactive groups that may be formed over the surface of silicon-derived ceramic materials that are processed in air or oxygen-rich atmospheres. Some authors have reported that the silane population, the acid–base properties and the potential to form hydrogen bridges are key factors to determine the potential toxicity of a pulverized solid [1]. It has been also reported that these active centers entail a chemical specificity similar to enzymes [2].

In several ceramic processing techniques, the materials must be employed as very fine powders or dispersed either in aqueous or organic solutions. The dispersion of powdered solids is controlled by the interaction energy among the constituent particles [3]. This interaction can be controlled by a deep knowledge of the surface properties of the solids and the use of polyelectrolytes [4]. The surface charge and chemical properties of the surface of any ceramic powder depend on both the chemical composition and synthetic procedure. For this reason, the required dispersant to process a determined ceramic powder or mixture must be specifically selected according to the surface characteristics. This statement is however questioned by several authors which assume that it is possible to reach a perfect dispersion of powdered ceramics by controlling several parameters such as the isoelectric point, the difference between the isoelectric point and the pH of the dispersion and acquiring the most adequate conformation of the polyelectrolyte to increase the stability of the particles [5]. Inorganic particles possess a high tendency to form aggregates and a poor capability to disperse in organic solvents, mainly due to their high surface energy. Some authors have used polyols or fatty acid to successfully disperse inorganic particles due to partial in situ polymerization of the surface functional groups of the particles and the organic segments of the solvent [6]. Nevertheless, inorganic fillers usually have specific gravities above two while the specific gravities of the polyols are generally around one, resulting in sedimentation of the suspensions after a certain period of time, especially when the solvents have the relatively low viscosities. In addition to this, because of this weak interaction between organic and inorganic surfaces, the use of inorganic fillers in organic matrices gives as a result composite materials with loose mechanical properties and thus the application of composite materials reinforced with ceramic powders is still minority. Attempts to improve the dispersion of ceramic particles into polymeric matrices involve the modification of surface properties. Among these modifications, physical changes are temporary and occurs via thick interfaces whereas the chemical modifications are fundamentally based on the use organic molecules used as coupling agents [7].

Wettability is the property of a fluid to adhere on the surface of a solid in the presence of another non-miscible fluid. The surface energy of a solid and the surface heterogeneities are the main factors that will determine the wettability of the solid. These properties can be determined through contact angle measurements or inverse gas–solid chromatography (IGC-ID). In the first case, the obtained results are exclusively macroscopic and represent the average surface energy of the material since the effect of surface roughness, porosity and particle size and shape are alleviated. IGC-ID provide more reliable results since the mentioned factors are excluded on the measurements and the most representative results refer to the active centers of the solid [8].

SiC particles possess a great technological interest due to their excellent mechanic properties at high temperatures, excellent thermal tolerance and resistance against oxidation and wear. SiC runs for an excellent candidate in polymer reinforcing but its main limitation is the high tendency to agglomerate. Interestingly, despite the low or medium surface energy values, it also presents intriguing characteristics as ceramic support in heterogeneous catalysis processes. In addition to the above mentioned characteristics, it is considered intrinsically inert but after chemical deposition of Fe, Ni or Co catalysts over the surface of the SiC particles, they have been tested in Fischer–Tropsch synthetic procedures [9]. Thanks to the high thermal conductivity, hot spots inside the reactor are avoided and thus, the selectivity against heavy hydrocarbon fuels is enhanced as a consequence of the minimization of thermal gradients. Nevertheless, the deposition of the metal catalyst on the surface of the SiC particles is acutely influenced by the nature of the catalyst precursor (acetate, chloride,

Table 1 – Properties of the studied SiC particles (S_{BET} refers to the specific surface area as determined by BET).

SiC sample ID	Pore diameter (μm)	Density (g/cm^3)	S_{BET} (m^2/g)	SiO_2 (%)	C_{free} (%)
SiC07	0.76	3.77 ± 0.02	3.8	0.09	0.12
SiC1	1.08	3.80 ± 0.01	1.6	0.25	0.1
SiC7	7.61	3.79 ± 0.01	0.9	0.1	0.3
SiC10	10.32	3.79 ± 0.01	0.3	0.16	0.06

carbonyl, etc.) due to its dispersion and interaction with the surface of the particles. Therefore, inertness or activity of SiC particles will depend on both upon milling and synthetic procedures [10,11]. Knowledge of the physical, chemical and thermal properties of SiC is then deciding for the use at high temperature or under harsh environments [12].

The surface properties of SiC are determined by the presence of the two atoms: Si atom is less electronegative than C, it forms weak bonds (except when highly electronegative atoms are involved), it is kinetically more reactive and possess higher atomic radius. Thus, the surface of SiC nanostructures (such as SiCNTs) is more reactive than the one of similar C-rich nanostructures (CNTs) and the thermal stability decreases as well [13]. Because of their enhanced reactivity, SiCNTs are able to adsorb quantitative amounts of H_2 and they are potential candidates for H_2 storage or as gas detectors [14].

Surface acid–basic properties also serve to describe the reactivity of the solids. NH_3 and H_2O are frequently used as probe molecules to experimentally determine the Lewis and Brönsted acidity or basicity since the binding energy of a particular active site serves as an estimation of the acidic strength [2,15]. It have been demonstrated that whilst thermal treatment of cristobalite induces a decrease of the surface energy, beyond 800 °C, SiC experiments a significant increase being even able to dissociate H_2O or NH_3 molecules [2]. The major part of these solids possess distinct active sites which can be subjected to selective doping in increase their activity [16]. In this sense, the substitution of a C or Si atom by Al, the interaction energy increases but it decreases if the substituting atom is B. This energy is higher if the substitution occurs in the C atom rather than in Si [17].

With all these concerns, we aim to shed light to the surface properties of different SiC by comparing two surface driven techniques such as IGC-ID and XPS. The former one informs about the surface composition whereas IGC-ID is focused on the description of the surface energy. The combined application of these two techniques will allow a deep knowledge of the overall parameters that will determine the reactivity and interactions of the surface of SiC ceramics in subsequent processes.

Experimental

SiC samples were provided by Advanced Thermal Devices, S.L. and employed as received. According to the preparation procedure, the differences between particles in terms of their oxidation state and carbon content depend upon both the location of the SiC crystals with respect to the electrode (for the application of the current) and the post-treatment cleaning processes. Particles nearer to the electrode are high-purity SiC whereas C or SiO_2 impurities are found in the particles produced in the furthest regions. The main characteristics of the studied samples are collected in Table 1.

Specific surface area was determined through N_2 adsorption at −176 °C (Micromeritics, Tristar, USA) after degassing the samples for 18 h at 200 °C under He flow. Particle size distribution was obtained in a Malvern Mastersizer S by measuring the angular variation in intensity of light scattered as a laser beam passes through a well dispersed sample.

For IGC-ID measurements, the chromatographic columns filled with the SiC particles were conditioned and degassed at 200 °C for 18 h under a continuous He flow fixed to 20 cm^3/min. The maximum compaction of the particles within the column was obtained through applying a vibration force during the filling process and thus, the diffusion of the adsorbate and the formation of preferential diffusion channels were minimized. The properties of the probe molecules used for the calculations of the surface energy parameters are collected in Table 2. Infinite dilution was achieved by injecting 0.1 μl of the adsorbate pre-heated for 1 h at 100 °C in a 1 l flask. The analysis temperature varied from 80 to 100 °C. A Perkin Elmer Autosystem fitted with a FID detector was used for the measurements.

Table 2 – Properties of the injected probe molecules.

Molecule		DN (kcal mol^{-1})	AN*	Character	$(h\nu_L)^{1/2}\alpha^*10^{49}$ (C$^{3/2}$ m^2 V$^{-1/2}$)
n-Pentane	C5	–	–	Neutral	8.10
n-Hexane	C6	–	–	Neutral	9.20
n-Heptane	C6	–	–	Neutral	10.30
n-Octane	C8	–	–	Neutral	11.45
Chloroform	CL	0	5.4	Acid	7.80
Benzene	BZ	0.1	0.17	Acid	8.60
Acetone	AC	17.0	2.5	Amphoteric	5.80
Ethyl acetate	EA	17.1	1.5	Amphoteric	7.90
Diethyl ether	DE	19.2	1.4	Basic	7.30
Tetrahydrofurane	THF	20.6	0.5	Basic	6.80

Both the injector and the detector were maintained heated to 250 °C in order to avoid undesirable molecule condensation.

XPS spectra were collected in a VG Escalab 200R spectrophotometer equipped with a hemispheric electronic analyzer and using monochromatic Mg K_α radiation as X ray source (1253.6 eV, 1 eV = 1.6022 × 10^{19} J). The spectrophotometer is fitted with Ag, Au and Cu internal standards for calibration in the full spectral range. For spectrometer calibration, the binding energies have been referenced to the Ag_{4d} peak and the line position C_{1s} was used as binding energy reference. SiC samples mounted in the sample holder were previously degassed at room temperature prior to be introduced into the analysis chamber. The pressure inside the analysis chamber was maintained constant at 3×10^{-9} mbar during the spectral acquisition. A compromise between resolution and acquisition time is obtained when a 20 eV step was used. The surface charge of the XPS spectra were corrected by applying a very small current over the samples by a FLOOD GUN emission system. C_{1s}, O_{1s} and Si_{2p} peaks were analyzed to determine the surface composition of the SiC materials. Binding energies were collected with a ±0.2 eV resolution.

Theory of IGC-ID

IGC-ID is a very versatile technique to characterize the surface properties of any solid material at a molecular scale. The technique is quite affordable, easy to handle and provide fast results except in highly energetic materials or in the presence of very fine pores (ultramicropores). The main parameter of IGC-ID is the retention time t_R of the probe molecule injected in the column containing the solid material. This retention time depend upon the interactions between the molecules of the probe and the active centers located at the surface of the solid. In the infinite dilution variation, the number of probe molecules passing through the column is very low and then, it can be considered that intermolecular interactions do not exist. The retention volume of the probe molecule can be calculated from the retention time t_R as following:

$$V_R = (t_R - t_0)F_0 \quad (1)$$

where t_0 is the retention time of a probe molecule that do not interact with the surface of the solid and F_0 the carrier flow. F_0 is a function of the compressibility of the carrier and the variation of the pressure along the column and must be corrected for each measuring temperature [18].

At infinite dilution, Henry's law applies since intermolecular interactions are disregarded. $-\Delta G_0^A$ is then related to the retention volume by Eq. (2)

$$-\Delta G_0^A = RT \ln V_R + K \quad (2)$$

being T the analysis temperature, R the gas constant and K is a constant that depends on the reference state. By analyzing the different $-\Delta G_0^A$ for the probe molecules collected in Table 2, the dispersive energy and the acid–base characteristic of the analyzed solid can be inferred.

The dispersive surface energy γ_s^d is calculated from the application of the Dorris–Gray equation [19]:

$$\gamma_S^d = {}^1\!/_{\gamma_{CH_2}} \left(-\Delta G_A^{CH_2}/2N_A\, a_{CH_2}\right)^2 \quad (3)$$

Here γ_{CH_2} is the surface energy of a hypothetic solid containing exclusively methylene groups, N_A refers to Avogadro's Number and a_{CH_2} is the surface area of a methylene group (0.06 nm^2). $-\Delta G_A^{CH_2}$ can be calculated from the slope of Eq. (2) when a series of *n*-alkanes with increased number of methylene groups are injected. By increasing the number of methylene groups in the probe molecule, the interaction of the vapor with the solid surface increases as well and thus, the positive slope corresponds to $\Delta G_A^{CH_2}$ in Eq. (3).

Lewis acid–base specific surface energy can be calculated from the specific interactions of different probe molecules with acid–base properties. Actually, the specific energy includes all sort of interactions such as polar interactions, hydrogen bonds and metallic or magnetic interactions but it does not account for the dispersive interactions, as commented before. Thus, the difference between the total free energy of the injected probe molecule and the line obtained in Eq. (2) (purely dispersive interactions) represents the contribution of the specific interactions ΔG^{SP}. The issue in question arises what is the most appropriate property of a molecule to determine the difference between the dispersive and specific energies. Among these properties, it is possible to select the vapor pressure, molecular area, molar polarization, Kovats index or topological molecular index [20]. In this work, we have considered the molar deformation polarization (α_0), as proposed by Donnet et al. [21] since it includes both the electronic (α_e) and atomic (α_a) polarizabilities. α_0 values for the probe molecules used in this work are collected in Table 2.

The value of the specific interaction, $-\Delta G_0^{SP}$, is calculated from the difference between the $-\Delta G_0^A$ value of the probe

Table 3 – Binding energies (eV) of the internal electrons and surface atomic ratios.

Muestra	C1s		O1s	Si2p		Si/C atom
	eV	%	eV	eV	%	
SiC07	283.2 284.9	70 30	533.5	101.1 103.1	74 26	0.97
SiC1	283.5 284.9	63 37	533.1	101.4 102.9	87 13	1.14
SiC7	283.1 284.9	62 38	532.7	101.0 103.1	81 19	0.70
SiC10	283.1 284.9	64 36	533.1	101.2 103.1	83 17	1.09

molecule and the straight line obtained after the injection of *n*-alkanes according to the selected property, α_0 [22]. Acid, k_A, and base, k_B, constants are calculated from Eq. (4) since DN and AN* values are tabulated in Table 2. In this work, we have selected the values recommended by Riddle and Fowkes since they exclude the Van der Waals contribution in the acid–base energy of the probe molecules [23].

$$\Delta G_0^{SP} = k_A DN + k_B AN^* \quad (4)$$

Results

The surface stoichiometry and composition of the SiC samples were analyzed by XPS (Table 3). The surface of the samples is slightly oxidized because of the milling process or the synthetic procedure, as deduced from the appearance of the O_{1s} signal in the spectra. This fact is a common characteristic of the SiC materials where it is detected the formation of silica or silicon oxycarbide due to intrinsic oxidation processes [24,25]. The peaks Si_{2p} and C_{1s} appear at 101 eV and 283 eV respectively and correspond to the unnoxidized Si and C atoms of the SiC. The binding energies of the Si–O and C–O bonds are shown in the spectra shifted to high energy values, specifically at 103 eV and 285 eV. These two weak signals confirms the formation of SiO_2-like species and the oxidation of the C atoms [26]. Fig. 1 shows the portion of the XPS spectra assigned to the Si_{2p} signal in each studied sample and Fig. 2 the spectra of the C_{1s} core level.

The bands appearing in the XPS spectra have been analyzed and convoluted by assuming a contribution of Gaussian–Lorentzian signals. The percentage area of each band has been obtained (Table 3) and from this value, the Si/C ratio of the surface has been calculated. From the results collected in Table 3 it can be concluded that in the samples SiC07, SiC1 and SiC10, the Si/C ratio is near the stoichiometric one but in the SiC7 sample (particle size = 7 μm), it exists an excess of C on the surface of the particles.

Further information of the surface properties of the SiC samples can be extracted from the IGC-ID analysis. Fig. 3 shows the variation of ΔG_0^A as a function of the number of C atoms in the probe molecule when the vapor interacts with the surface of the SiC10 sample at different temperatures. Fig. 4 represents this interaction for the different SiC samples conditioned at the same temperature.

In all the cases, the ΔG_0^A values can be fitted to a straight line ($1 < r^2 < 0.999$) indicating that dispersive interactions dominate the values of the surface free energies when the different alkanes are injected into the columns filled with the SiC. From these lines, and by applying Eq. (3), the dispersive surface energy of the SiC samples are calculated and collected in Table 4. Extrapolation to 25 °C was carried out to determine the dispersive energy at this temperature.

The results in Table 4 show an increase of the dispersive surface energy values as decreasing the particle size. Since the dispersive energy represents the ability of the electron cloud to create a dipole on it, this capability increases when decreases the particle size since the atomic bonds are more distorted in low-sized particles.

The calculated values of the specific interactions with the SiC10 sample at 80 °C are shown in Fig. 5. In this representation it can be appreciated that since the *n*-alkanes interact

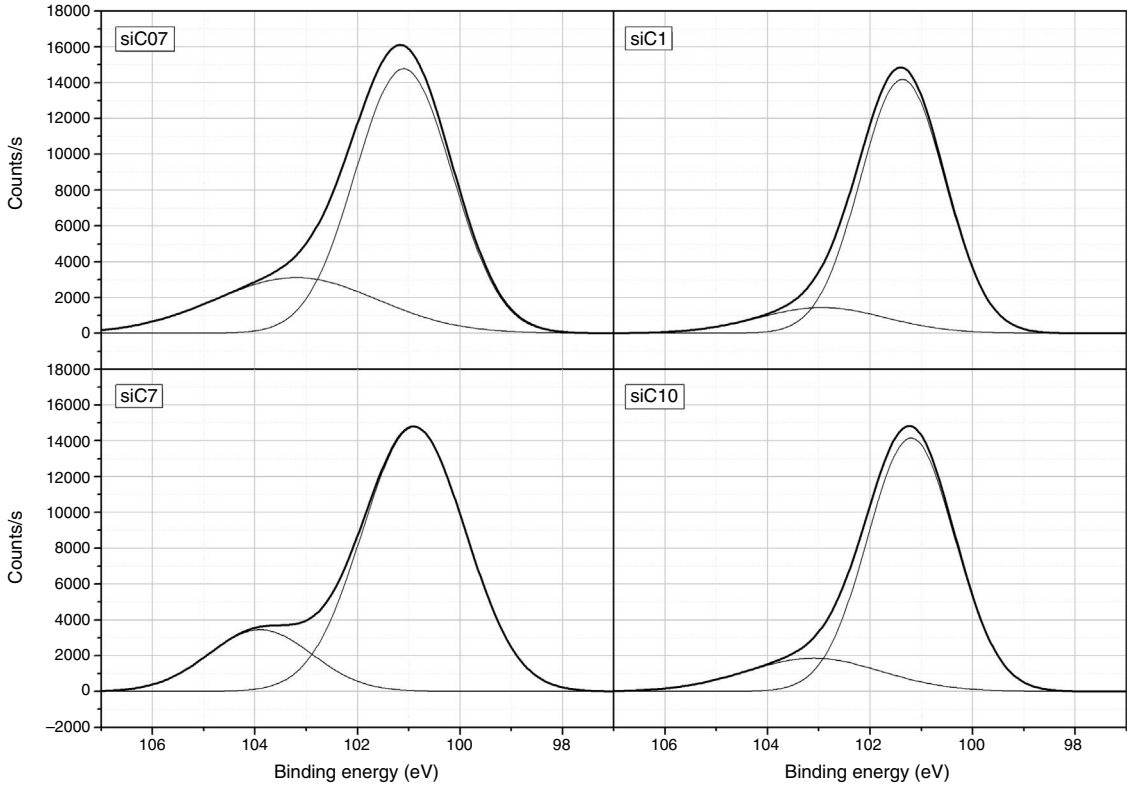

Fig. 1 – XPS spectra of the studied samples in the range corresponding to the Si_{2p} signal.

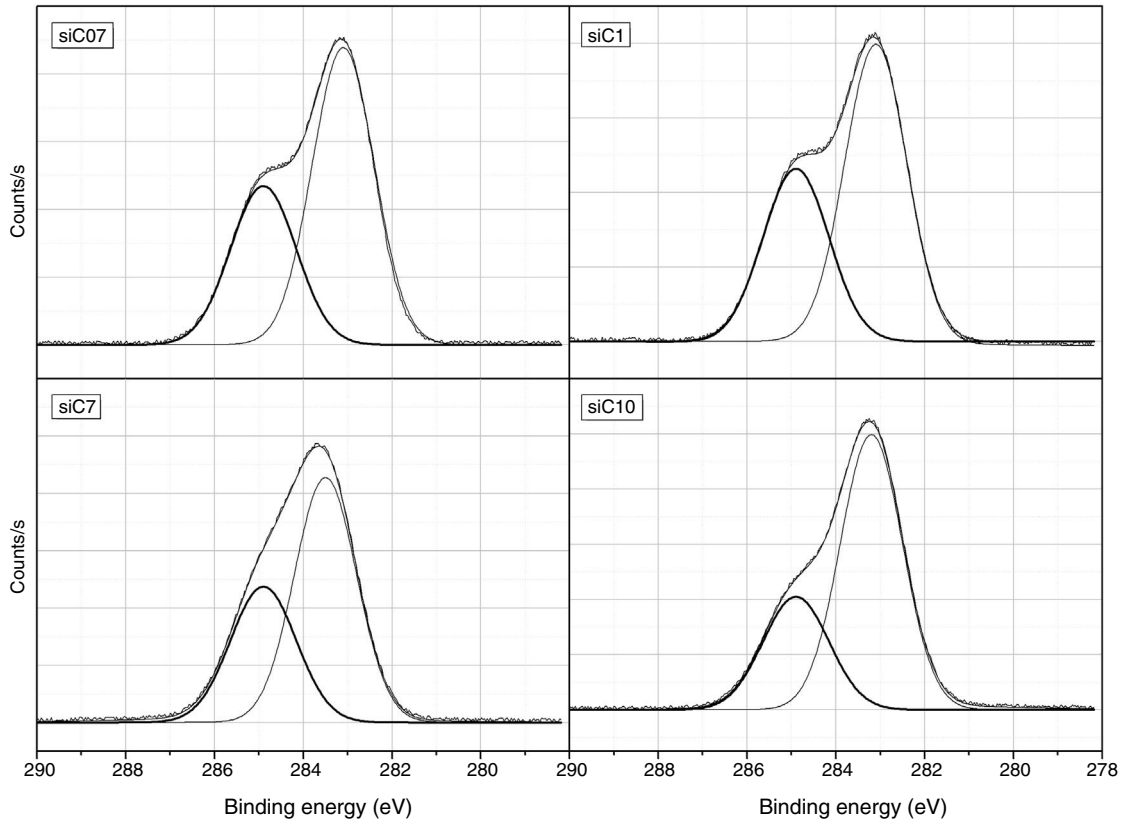

Fig. 2 – XPS spectra of the studied samples in the range corresponding to the C_{1s} signal.

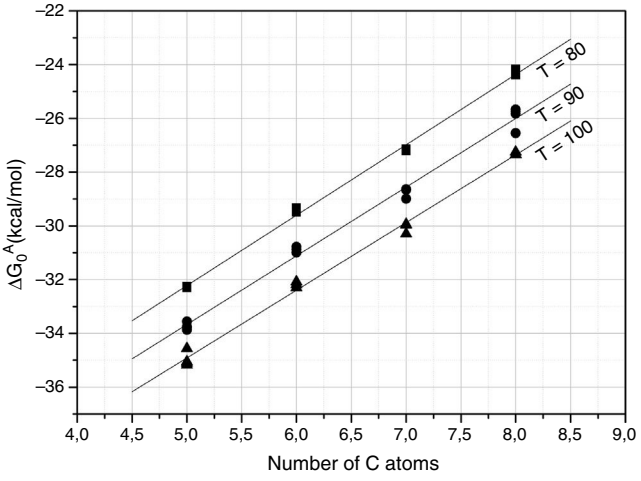

Fig. 3 – ΔG_0^A values calculated from Eq. (1) of the probe molecules injected in the chromatographic column filled with SiC10 and conditioned at 80, 90 and 100 °C.

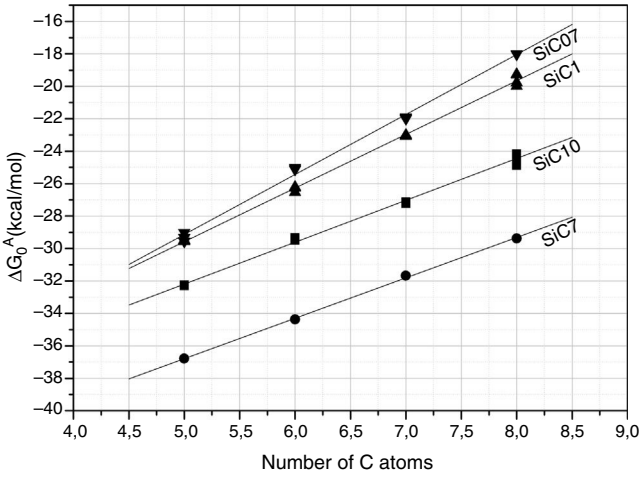

Fig. 4 – ΔG_0^A values calculated from Eq. (1) of the probe molecules injected in the chromatographic column filled with the different SiC samples and conditioned at 80 °C.

exclusively via dispersive forces, the values can be fitted to straight lines as a function of the molar deformation polarization. Nevertheless, the ΔG_0^A values of the probe molecules with a specific component falls away from this line to a distance depending upon the strength of the acid–base interaction with the SiC surface. The distance of each specific probe molecule with the *n*-alkane line corresponds to the specific interaction ΔG_0^{SP}. Plots of ΔG_0^{SP} vs AN* and DN allow the calculation of the acid–base constant of each SiC simple through the application of Eq. (4). This representation can be found in Fig. 6, where it is observed that all the SiC samples present similar acid–base constant values since all the straight lines possess similar slopes and y-intercepts as well. k_A and k_B values are collected in Table 5.

Although the k_A and k_B values are very similar in all the samples, there exist some differences attributed to the different surface composition and stoichiometry. These differences

Table 4 – Dispersive energies of the surface of the different SiC studied in this work.

Sample	Temperature (°C)			
	80	90	100	25
SiC07	60.90	57.32	54.80	77.52
SiC1	58.21	54.65	53.36	71.17
SiC7	33.45	31.54	30.87	40.35
SiC10	35.86	34.51	32.72	44.55

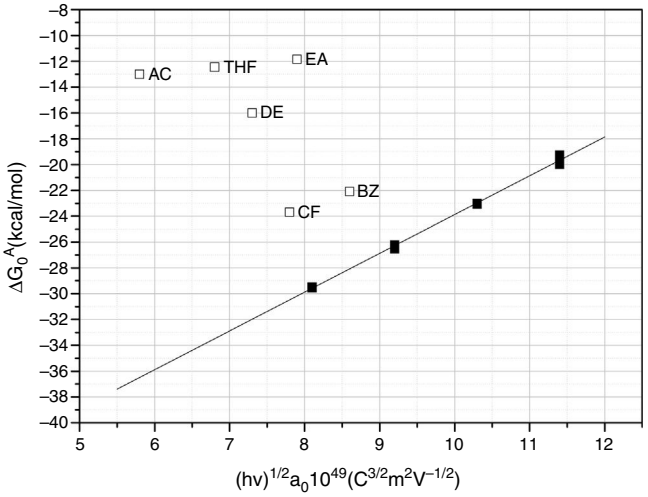

Fig. 5 – Variation of ΔG_0^A values for the polar and non polar molecules in the simple SiC10.

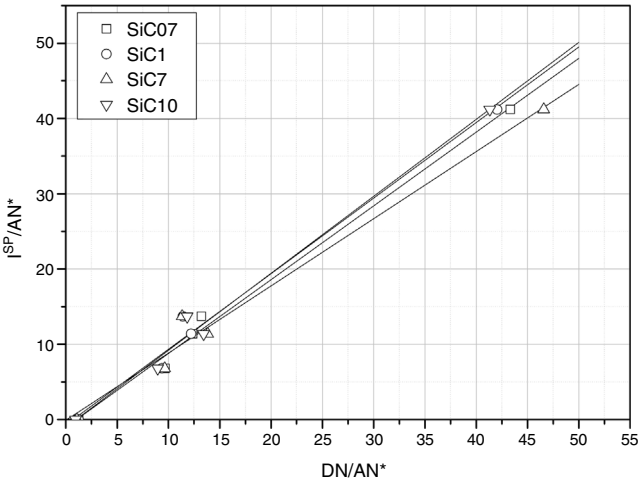

Fig. 6 – Determination of k_A and k_B from the I^{SP} for the different SiC samples.

will be discussed and correlated with the XPS results (Table 3) in the next section.

Discussion

Bulk characterization techniques, such as FT-IR and Raman spectroscopies or X-ray diffraction (not shown here) do not throw any relevant information about the different surface properties of similar samples with different particle size. Surface-driven characterization techniques such as XPS or IGC-ID should be therefore exploded to correlate the different behavior of the materials during processing. As depicted in the previous section, both the XPS or IGC-ID have shown slight differences among the studied samples which can be correlated with the particle size and composition. XPS results (Table 3) indicate that all the samples are slightly oxidized and possess SiO_2 distributed all over their surfaces. As shown in Fig. 1, the fundamental line of Si_{2p} can be decomposed in two signals. The first one appears around 101.2 eV (±0.2) and the other line is shifted to 103.1 eV (±0.2) suggesting that the Si atoms are in two different oxidation states. The first peak, at low binding energy values, corresponds to the Si–C bond and its intensity is considerably higher than the second peak, appearing at 103.1 eV which is assigned to oxidized Si4+ atoms bonded to O. The oxidized Si atoms form SiO_2-like areas through Si–O bonds [24,25] or as in silicon oxycarbide materials, via C–Si–O bonds as suggested by some other authors [26].

Table 5 – Acid and base constant values calculated for the different SiC samples.

	SiC07	SiC1	SiC7	SiC10
k_A	1.01	0.98	1.10	1.00
k_B	1.15	0.90	0.40	1.15
$k_A + k_B$	2.16	1.88	1.50	2.15
k_B/k_A	1.14	0.92	0.36	1.15

Besides the presence of some SiO_2 over the surface of the SiC materials, the analysis of the C_{1s} signal of the XPS spectra (Table 3) also show that the C atom is in different oxidation states. In this case, the main signal is located at 283.2 eV (±0.2) and corresponds to the C–Si bond of SiC whereas at 284.9 eV (±0.2) it is also found a small signal that could be assigned either to C–C bonds or C–Si–O bonds. No C–O containing groups are detected in the XPS spectra since the most intense signal that could be attributed to these species is close to 286 eV [25] and no traces of any prominence around this range are detected in the spectra. The analysis of the bands attributed to both Si_{2p} and C_{1s} signals indicate that the surface Si/C atomic ratio is close to the stoichiometric one except for the sample SiC7 that contains more C than expected. The surface stoichiometry seems to be independent of the particle size since the sample containing the more amount of C is the one whose main particle size is about 7 μm.

The surface analysis by means of IGC-ID also reveals some differences in the surface properties and composition which are independent of the particle size. The values of the dispersive surface energy, γ_s^d (Table 4) decrease as increasing the particle size with the exception of the sample SiC7 whose value is minor than the expected. This result can be correlated with the XPS measurements. The dispersive component of the surface free energy is directly related to the atomic density of the surface and it is proportional to the molar polarization and ionization energy as well. Therefore, γ_s^d values are quite sensitive to surface changes. The increase of γ_s^d with the decrease of the particle size is probably due not only to changes in the chemical composition but the milling process as well [27]. Nevertheless, the encountered γ_s^d value of SiC7 is lower than the one found in the sample SiC10, a result that

may be directly related to the lower Si/C ratio found in the XPS analysis. A similar result was found in silicon oxycarbide materials prepared by sol–gel method where the increase of the free carbon amount and the number of carbons bonded in C–Si–O structures lead to a decrease in the γ_s^d [28].

The encountered γ_s^d values for the SiC materials are slightly higher than the values reported for silica or quartz [20,29,30] and they are considerably lower than the ones reported for different carbon allotropes [31,32]. In general, microporous and graphitic carbons, nanotubes and nanofibers included, possess high γ_s^d values due to strong interactions with the probe molecules and the presence of defects and surface heterogeneities. By increasing the amount of surface heterogeneities, the γ_s^d acquires higher values. No reported studies have been found in the literature regarding the effect of the surface heterogeneities on the γ_s^d values of the SiC materials, but it is expected that its behavior should be similar to other ceramic or crystalline materials whose values are comprised between 50 and 100 mJ/m^2 [20], and similar to the ones calculated in this work.

With regard to the acid–base properties of the analyzed SiC samples, the obtained values indicate that the materials possess an amphoteric character as the presence of two types of active centers suggest. This character is in perfect agreement with the surface chemical composition of the materials obtained by XPS. The global acid–base energy value, i.e. $k_A + k_B$, is minimum for the SiC7 sample that is also the sample that presented the lowest γ_s^d value and the highest amount of C atoms in the surface of the material. This excess of C must be necessarily related with the high energy active centers, either the dispersive or Lewis acid–base sites. With the exception of this sample SC7, the $k_A + k_B$ values of the three SiC samples are higher than the values reported of silica or quartz [28] indicating that the surfaces are more energetic than the SiO_2-based materials. In general, in the materials based on silica, the k_B/k_A ratio is lower than 0.50 [33] indicating their acidic nature. The ratio k_B/k_A encountered for many glasses increases up to 1.18 because they are amphoteric materials [34]. On contrary, for graphitic materials this ratio is around 0.7, but for some other carbon-based materials such as carbon nanofibers or nanotubes, values as low as 0.23 or 0.30 respectively are reported [35–37].

As mentioned before, the sample SiC7 presents the lowest k_A/k_B ratio. The value $k_B/k_A = 0.36$ suggests that the majority of the active site centers are blocked or occupied by carbon atoms, as previously demonstrated in the discussion of the XPS results. Similar surface characteristics with very low k_B/k_A values were found in SiOC materials with different types of oxidic and free carbon atoms [28]. It can be also proved that for the other three samples that possess a stoichiometric Si/C ratio, not only the $k_A + k_B$ values but also the k_B/k_A ratios are also are higher than in the silica-based materials indicating highly energetic surfaces covered with Lewis basic sites, a fact that is in complete agreement with the isoelectric point of the materials. The higher basicity of the materials, as determined for IGC-ID, corresponds to a higher isoelectric point [29,38] and the SiC materials studied in this work present a isoelectric point which is close to the silica, whereas for pure and unoxidized SiC, this point is close to 3–4 [5,39–41].

Conclusions

In this work we have demonstrated the capability of the XPS and IGC-ID techniques to evaluate both the chemical composition and the surface energy of the materials and the necessity to use both techniques to complement the information extracted from the analysis. All the analyzed SiC materials present some degree of oxidation over the surface of the material that courses with the formation of SiO_2 and Si/C ratios close to the stoichiometry except for the sample sized to 7 μm that presented an excess of C on the surface of the particles. The surface energy values obtained through the analysis of IGC-ID chromatograms plenty correspond to the XPS spectra. The lowest dispersive surface energy is found in the low-sized particles as soon as the Si/C ratios remain constant. In the sample with an excess of surface C, the dispersive surface energy decreases significantly indicating that the major part of the active sites are blocked with the carbon atoms. The overall surface energy of the materials as well as the basic component of the energy are higher than silica-derived materials, which is in perfect agreement to a higher isoelectric point of the SiC-based materials with respect to SiO_2.

Acknowledgements

This work has been financially supported by Spanish Ministry of Economics and Competitiveness (MAT2016-76516-R). Financial support from Fundacion General CSIC (Programa Comfuturo) is also acknowledged.

REFERENCES

[1] P. Hobza, J. Sauer, C. Morgeneyer, J. Hurych, R. Zahradnik, Bonding ability of surface sites on silica and their effect on hydrogen bonds. A quantum-chemical and statistical thermodynamic treatment, J. Phys. Chem. 85 (1981) 4061–4067.
[2] B. Fubini, V. Bolis, A. Cavenago, P. Ugliengo, Ammonia and water as probes for the surface reactivity of covalent solids: cristobalite and silicon carbide, J. Chem. Soc. Faraday Trans. 88 (1992) 277–289.
[3] I.A. Aksay, F. Lange, B.I. Davis, Uniformity of Al_2O_3–ZrO_2 composites by colloidal filtration, J. Am. Ceram. Soc. 66 (1983).
[4] E. Lidén, L. Bergström, M. Persson, R. Carlsson, Surface modification and dispersion of silicon nitride and silicon carbide powders, J. Eur. Ceram. Soc. 7 (1991) 361–368.
[5] R.S. Premachandran, S.G. Malghan, Dispersion characteristics of ceramic powders in the application of cationic and anionic polyelectrolytes, Powder Technol. 79 (1994) 53–60.
[6] Y. Chen, S. Zhou, H. Yang, L. Wu, Structure and properties of polyurethane/nanosilica composites, J. Appl. Polym. Sci. 95 (2005) 1032–1039.
[7] M.C. Bautista, J. Rubio, J.L. Oteo Mazo, El proceso de Organofilización de Vidrios para su aplicación en Materiales Compuesto, Bol. Soc. Esp. Cerám. Vidr. 30 (1991) 81–91.
[8] G. Buckton, Contact angle, adsorption and wettability – a review with respect to powders, Powder Technol. 61 (1990) 237–249.

[9] H.M. Torres Galvis, A.C.J. Koeken, J.H. Bitter, T. Davidian, M. Ruitenbeek, A.I. Dugulan, K.P. de Jong, Effect of precursor on the catalytic performance of supported iron catalysts for the Fischer–Tropsch synthesis of lower olefins, Catal. Today 215 (2013) 95–102.
[10] M.P. Rosynek, C.A. Polansky, Effect of cobalt source on the reduction properties of silica-supported cobalt catalysts, Appl. Catal. 73 (1991) 97–112.
[11] S. Sun, N. Tsubaki, K. Fujimoto, The reaction performances and characterization of Fischer–Tropsch synthesis Co/SiO_2 catalysts prepared from mixed cobalt salts, Appl. Catal. A: Gen. 202 (2000) 121–131.
[12] Y.T. Yang, R.X. Ding, J.X. Song, Transport properties of boron-doped single-walled silicon carbide nanotubes, Phys. B: Condens. Matter 406 (2011) 216–219.
[13] V.E. Chelnokov, A.L. Syrkin, High temperature electronics using SiC: actual situation and unsolved problems, Mater. Sci. Eng.: B 46 (1997) 248–253.
[14] L. Wang, Adsorption of formaldehyde (HCOH) molecule on the SiC sheet: a first-principles study, Appl. Surf. Sci. 258 (2012) 6688–6691.
[15] H. Yao, Y. Chen, Y. Wei, Z. Zhao, Z. Liu, C. Xu, A periodic DFT study of ammonia adsorption on the V_2O_5 (001), V_2O_5 (010) and V_2O_5 (100) surfaces: Lewis versus Brönsted acid sites, Surf. Sci. 606 (2012) 1739–1748.
[16] A. Joshi, A. Rammohan, Y. Jiang, S. Ogunwumi, Density functional theory (DFT) study of the interaction of ammonia with pure and tungsten–doped ceria, J. Mol. Struct.: THEOCHEM 912 (2009) 73–81.
[17] A. Ahmadi Peyghan, S. Amir Aslanzadeh, M. Noei, A density functional study on the acidity properties of pristine and modified SiC nano-sheets, Phys. B: Condens. Matter 443 (2014) 54–59.
[18] R. Ho, J.Y.Y. Heng, A review of inverse gas chromatography and its development as a tool to characterize anisotropic surface properties of pharmaceutical solids, KONA Powder Part. J. 30 (2013) 164–180.
[19] G.M. Dorris, D.G. Gray, Adsorption of n-alkanes at zero surface coverage on cellulose paper and wood fibers, J. Colloid Interface Sci. 77 (1980) 353–362.
[20] S. Mohammadi-Jam, K.E. Waters, Inverse gas chromatography applications: a review, Adv. Colloid Interface Sci. 212 (2014) 21–44.
[21] J. Donnet, S. Park, H. Balard, Evaluation of specific interactions of solid surfaces by inverse gas chromatography, Chromatographia 31 (1991) 434–440.
[22] C. Saint Flour, E. Papirer, Gas–solid chromatography: a quick method of estimating surface free energy variations induced by the treatment of short glass fibers, J. Colloid Interface Sci. 91 (1983) 69–75.
[23] F.L. Riddle, F.M. Fowkes, Spectral shifts in acid–base chemistry. 1. Van der Waals contributions to acceptor numbers, J. Am. Chem. Soc. 112 (1990) 3259–3264.
[24] N.K. Huang, D.Z. Wang, Q. Xiong, B. Yang, XPS study of hydrogen permeation effect on SiC–C films, Nucl. Instrum. Methods Phys. Res. Sect. B: Beam Interact. Mater. Atoms 207 (2003) 395–401.
[25] Y.Y. Wang, K. Kusumoto, C.J. Li, XPS analysis of SiC films prepared by radio frequency plasma sputtering, Phys. Proc. 32 (2012) 95–102.
[26] E. Bouillon, F. Langlais, R. Pailler, R. Naslain, F. Cruege, P. Huong, J. Sarthou, A. Delpuech, C. Laffon, P. Lagarde, Conversion mechanisms of a polycarbosilane precursor into an SiC-based ceramic material, J. Mater. Sci. 26 (1991) 1333–1345.
[27] E. Papirer, J.-M. Perrin, B. Siffert, G. Philipponneau, J.-M. Lamerant, The influence of grinding on the surface properties of α-aluminas, J. Colloid Interface Sci. 156 (1993) 104–108.
[28] A. Tamayo, R. Peña-Alonso, J. Rubio, R. Raj, G.D. Sorarù, J.L. Oteo, Surface energy of sol gel-derived silicon oxycarbide glasses, J. Am. Ceram. Soc. 94 (2011) 4523–4533.
[29] C.-W. Won, B. Siffert, Preparation by sol–gel method of SiO_2 and mullite ($3Al_2O_3$, $2SiO_2$) powders and study of their surface characteristics by inverse gas chromatography and zetametry, Colloids Surf. A: Physicochem. Eng. Aspects 131 (1998) 161–172.
[30] A. Khalfi, E. Papirer, H. Balard, H. Barthel, M.G. Heinemann, Characterization of silylated silicas by inverse gas chromatography: modelization of the poly(dimethylsiloxane) monomer unit/surface interactions using poly(dimethylsiloxane) oligomers as probes, J. Colloid Interface Sci. 184 (1996) 586–593.
[31] H. Balard, D. Maafa, A. Santini, J.B. Donnet, Study by inverse gas chromatography of the surface properties of milled graphites, J. Chromatogr. A (2008) 173–180, 1198–1199.
[32] E. Papirer, E. Brendle, F. Ozil, H. Balard, Comparison of the surface properties of graphite, carbon black and fullerene samples, measured by inverse gas chromatography, Carbon 37 (1999) 1265–1274.
[33] M. Kimura, K. Nakamura, K. Tsutsumi, Surface free energies of silica fillers and their relation to the adsorption of poly(ethylene terephthalate), J. Colloid Interface Sci. 279 (2004) 509–514.
[34] U. Panzer, H.P. Schreiber, On the evaluation of surface interactions by inverse gas chromatography, Macromolecules 25 (1992) 3633–3637.
[35] E. Brendlé, E. Papirer, A new topological index for molecular probes used in inverse gas chromatography for the surface nanorugosity evaluation, J. Colloid Interface Sci. 194 (1997) 207–216.
[36] J. Schultz, L. Lavielle, Interfacial properties of carbon-fiber epoxy matrix composites, ACS Symp. Ser. 391 (1989) 185–202.
[37] X. Zhang, D. Yang, P. Xu, C. Wang, Q. Du, Characterizing the surface properties of carbon nanotubes by inverse gas chromatography, J. Mater. Sci. 42 (2007) 7069–7075.
[38] C.H. Sun, J.C. Berg, A review of the different techniques for solid surface acid–base characterization, Adv. Colloid Interface Sci. 105 (2003) 151–175.
[39] B.P. Singh, J. Jena, L. Besra, S. Bhattacharjee, Dispersion of nano-silicon carbide (SiC) powder in aqueous suspensions, J. Nanopart. Res. 9 (2007) 797–806.
[40] Y. Hirata, K. Miyano, S. Sameshima, Y. Kamino, Reaction between SiC surface and aqueous solutions containing Al ions, Colloids Surf. A: Physicochem. Eng. Aspects 133 (1998) 183–189.
[41] L. Saravanan, S. Subramanian, A.B.V. Kumar, R.N. Tharanathan, Surface chemical studies on SiC suspension in the presence of chitosan, Ceram. Int. 32 (2006) 637–646.